



PROCUREMENT EXECUTIVE, MINISTRY OF DEFENCE

AERONAUTICAL RESEARCH COUNCIL

REPORTS AND MEMORANDA

Application of Head's Entrainment
Method to the Prediction of Turbulent Boundary
Layers and Wakes in Compressible Flow

By J. E. GREEN

Aerodynamics Dept., R.A.E., Farnborough

RECEIVED
AERONAUTICAL RESEARCH COUNCIL
FARNBOROUGH

LONDON: HER MAJESTY'S STATIONERY OFFICE

1976

£2.90 NET

Application of Head's Entrainment Method to the Prediction of Turbulent Boundary Layers and Wakes in Compressible Flow

By J. E. GREEN

Aerodynamics Dept., R.A.E., Farnborough

*Reports and Memoranda No. 3788**
April, 1972

Summary

Details are given of an adaptation of Head's entrainment method to compressible flow which has been in use in R.A.E. since 1967. This version is a simplification of an earlier application of the entrainment method in compressible flow, and one which is believed internally consistent and reliable over a wider range of Mach numbers than its predecessor. The main feature of the method is that it has been 'tied' to the flat plate skin-friction correlation of Spalding and Chi, so that at least its accuracy in zero pressure gradient is assured. Other innovations are the introduction of a simple explicit two-parameter approximation to two more elaborate but implicit skin-friction relations, and the extension of the method to treat aerofoil wakes. Comparisons with experiment are shown to support these extensions. Finally, in Appendices, some further but as yet untried refinements of the method are presented and, in particular, a tentative treatment of compressible flows with heat transfer is given.

* Replaces R.A.E. Technical Report 72079—A.R.C. 34 052

LIST OF CONTENTS

1. Introduction
2. The Prediction Method for Incompressible Flow
 - 2.1. Basic equations
 - 2.2. Skin-friction relations
 - 2.3. Entrainment and shape-parameter relations
 - 2.4. Treatment of wakes
3. The Method for Compressible Flows
 - 3.1. Basic equations
 - 3.2. Skin-friction relations
 - 3.3. Other auxiliary relations
 - 3.4. Summary of method
4. Comparisons with Experiment
5. Conclusions

List of Symbols

References

Appendix A Application to compressible flows with heat transfer

Appendix B Some variations on the basic method

Illustrations—Figs. 1 to 11

Detachable Abstract Cards

1. Introduction

This Report describes an integral method for predicting the behaviour of turbulent boundary layers in two-dimensional and axisymmetric, compressible flows. The method has been in use at R.A.E. since 1967. It was developed in order to provide the kind of quick yet reasonably accurate predictions of boundary-layer growth that are needed in parametric studies of flow fields which contain significant viscous effects. A principal aim during its development was to achieve simplicity and internal consistency without sacrificing accuracy to any important degree.

In recent years there has been much emphasis on the need for greater sophistication in predicting turbulent boundary layers. Nevertheless, there are many situations of practical importance—for example, attached flow about aerofoil sections of conventional design—in which the method described here is as accurate as most of the recent, more elaborate treatments.

The present method was developed from that devised by Head¹ in which boundary-layer growth in incompressible flow was predicted by the simultaneous forward integration of the momentum-integral and entrainment equations. In a previous paper², the writer took the physical arguments which Head had put forward concerning the mechanism of entrainment and applied them directly to compressible flows. Hence, a prediction method was derived which differed appreciably from, and was considered superior to, an alternative treatment derived at the same time in which Head's original method was used in conjunction with a compressibility transformation. What is described here is a simplification of the better of the two methods of this earlier paper.* It makes no recourse to compressibility transformations, and has been formulated in such a way that, in flows with zero pressure gradient, the predicted skin friction agrees with that given by the empirical relation of Spalding and Chi³. By this means, it is believed, a realistic first-order allowance for the effects of compressibility is assured.

To make the method rapid without losing accuracy, explicit analytic approximations have been obtained to represent the flat-plate skin-friction relation of Spalding and Chi and the skin-friction relation derived by Thompson⁴ from his two-parameter family of velocity profiles. To treat wakes, the empirical expression for the entrainment coefficient is modified so that, far downstream of the trailing edge, the streamwise variation of shape parameter accords with that observed by Townsend⁵ in the far wake of a circular cylinder.

Comparisons between the predictions of the method and some experimentally observed boundary-layer developments are presented to illustrate its general accuracy, and also its shortcomings in more taxing situations. The potential and limitations of the method are discussed in the light both of these comparisons and of the 1968 conference at Stanford⁶ on the prediction of turbulent boundary layers.

The method described in the main text is restricted to adiabatic flow. However, an extension of the method to treat flows with heat transfer is given in Appendix A and a later development of the basic method, such that it predicts equilibrium flows more accurately, together with a simpler and probably more accurate skin-friction relation, are presented in Appendix B. Neither of these methods have been tested against experiment to any degree, which is why discussion of them is confined to Appendices.

2. The Prediction Method for Incompressible Flow

2.1. Basic Equations

We are concerned either with two-dimensional flows or with axisymmetric flows about a body of diameter $2r$. We define coordinates x and y along and normal to the surface, with corresponding velocity components u and v , we write density ρ and shear stress τ , and denote conditions at the wall and just outside the edge of the boundary layer by suffixes w and e respectively. Then, provided the thickness of the boundary layer is negligible compared with r , the parameters which enter the analysis are:

* After the preliminary draft of this Report had been written, Sumner and Shanebrook published a method²⁸ very similar to the present one and derived with the same intention of simplifying the author's previous method. The main difference between the two treatments is that the present one is explicitly 'tied' to the boundary layer on a flat plate.

overall boundary-layer thickness	$\delta = y$ at $\frac{u}{u_e} = 0.995$,	}	(1)
displacement thickness	$\delta^* = \int_0^\infty \left(1 - \frac{u}{u_e}\right) dy$,		
momentum thickness	$\theta = \int_0^\infty \frac{u}{u_e} \left(1 - \frac{u}{u_e}\right) dy$,		
mass flow thickness	$\Delta = \int_0^\delta \frac{u}{u_e} dy = \delta - \delta^*$,		
shape parameters	$\left. \begin{aligned} H &= \delta^*/\theta \\ H_1 &= \Delta/\theta \end{aligned} \right\}$,		
skin-friction coefficient	$C_f = \frac{\tau_w}{\frac{1}{2}\rho u_e^2}$,		
entrainment coefficient	$C_E = \frac{1}{r\rho_e u_e} \frac{d}{dx} \left(r \int_0^\delta \rho u dy \right)$ $= \frac{1}{r u_e} \frac{d}{dx} (r u_e \Delta)$.		

The parameters of greatest practical interest are the displacement and momentum thicknesses, and the skin-friction coefficient. The problem as posed here is; given the boundary-layer properties at some initial station and the distribution, downstream of that station, of free-stream velocity u_e , what is the corresponding distribution of θ , δ^* and C_f ? Head's proposal¹ was that boundary-layer growth should be predicted by the simultaneous forward integration of the von Karman momentum integral equation, which in axisymmetric flows may be written:

$$\frac{d\theta}{dx} = \frac{C_f}{2} - (H+2) \frac{\theta}{u_e} \frac{du_e}{dx} - \frac{\theta}{r} \frac{dr}{dx} \quad (2)$$

and the entrainment equation, an expression for the streamwise rate of change of the mass flow thickness, which in axisymmetric flow may be written:

$$\frac{d\Delta}{dx} = C_E - \frac{\Delta}{u_e} \frac{du_e}{dx} - \frac{\Delta}{r} \frac{dr}{dx} \quad (3)$$

This last equation is, in fact, simply a rearrangement of the definition of C_E given in equations (1). Writing $\Delta = H_1\theta$, and substituting for $d\theta/dx$ from equation (2), it may also be written as a rate equation for the shape parameter H_1 ,

$$\theta \frac{dH_1}{dx} = C_E - H_1 \left(\frac{C_f}{2} - (H+1) \frac{\theta}{u_e} \frac{du_e}{dx} \right), \quad (4)$$

in which form terms involving the body radius do not appear.

To integrate these equations, it is necessary to express the parameters H , C_E and C_f in terms of H_1 , θ and the local properties of the external flow. Head postulated unique relationships between the entrainment coefficient and the two shape parameters, and obtained empirical correlations in the forms $H(H_1)$ and $C_E(H_1)$. To determine the skin-friction coefficient, he employed the formula of Ludwig and Tillmann⁷ which gives $C_f(H, R_\theta)$, where R_θ is Reynolds number based on momentum thickness. In the present method, essentially the same assumptions are made. The empirical relations used, which differ slightly from the ones originally used by Head, are given in the following sections.

2.2. Skin-Friction Relations

Although our principal concern is the prediction of boundary-layer growth in flows with pressure gradients, the present method has been formulated with the case of constant-pressure flow as a main reference point.

This class of flow has been widely investigated at both subsonic and supersonic speeds, and its properties are reasonably well established over a wide range of Mach numbers. Consequently, by 'tying' the method to constant pressure flows, a fairly realistic first-order allowance was built into it for the effects of compressibility.

It was convenient to do this by introducing the properties of flat-plate boundary layers into the analysis in an explicit form. In treating compressible flows, the empirical correlation of Spalding and Chi was used to determine the influence of compressibility on skin-friction. Therefore, for consistency, their proposed relation between C_f and R_θ in incompressible constant-pressure flow was also adopted. However, since this relation did not allow C_f to be expressed explicitly as a function of R_θ , it was not in the interests of speed to use it directly in the prediction method. Instead, the table of C_f versus R_θ given by Spalding and Chi was curve-fitted with the simple relation

$$C_{f_0} = \frac{0.012}{\log_{10} R_\theta - 0.64} - 0.00093 \quad (5)$$

which, for R_θ up to 10^5 , lies within $\frac{1}{2}$ per cent of the tabulated values of C_f . Suffix 0 denotes flat-plate properties.

Then, taking the Clauser⁸ shape parameter G to be constant at 6.8 on a flat plate, the shape parameter H_0 was obtained as

$$H_0 = 1 / \left(1 - 6.8 \sqrt{\frac{C_{f_0}}{2}} \right). \quad (6)$$

The variation of H_0 with R_θ , as given by equations (5) and (6), is compared in Fig. 1 with various other correlations derived from Refs. 3 and 4 (together) and 9, 10 and 11. Equations (5) and (6) are seen to be roughly an average of the other correlations.

For flows with pressure gradients, C_f is no longer a function of Reynolds number only. It is usually accepted, however, that only one further parameter need be introduced and, hence, that a unique relation may be obtained between C_f , some shape parameter of the velocity profile, and Reynolds number based on some boundary-layer thickness parameter. The early formula of Ludwig and Tillmann⁷ was in the convenient form $C_f(H, R_\theta)$, but the later, more refined treatments by, for example, Thompson⁴ and Nash and Macdonald¹¹ have not yielded explicit relations for C_f . For the present purpose an expression was sought which gave C_f explicitly and which at the same time, introduced the properties C_{f_0} and H_0 of the flat-plate boundary layer with the same value of R_θ . In fact, it was found that values of C_f and H normalised with respect to flat-plate values at the same R_θ were well correlated by the simple expression

$$\left(\frac{C_f}{C_{f_0}} + 0.5 \right) \left(\frac{H}{H_0} - 0.4 \right) = 0.9. \quad (7)$$

In Fig. 2 this relation is compared with the less direct ones put forward by Thompson and Nash and Macdonald (in each case defining C_{f_0} by equation (5) and accepting whatever value of H_0 this produced). It will be seen that, except for values of H approaching separation, the form of the correlation comes near to eliminating not only the differences between the two authors (e.g. at $R_\theta = 10^5$ and $H = 1.28$ Thompson's curves give C_f as 1.8×10^{-3} , Nash and Macdonald's tabulations as 1.7×10^{-3}), but also the influence of Reynolds number. Near separation, no two-parameter skin-friction relation is wholly reliable because pressure gradients are usually large and have an appreciable effect on the shape of velocity profiles. At the same time, because it is small, skin friction in the vicinity of separation has very little effect on boundary-layer development. The discrepancies apparent in Fig. 2 for $H/H_0 > 1.6$ were therefore thought to be relatively unimportant and, for all practical purposes, equation (7) was considered a satisfactory engineering approximation.

2.3. Entrainment and Shape-Parameter Relations

To complete the method for incompressible flow, relations were needed for C_E and H as functions of H_1 (and, possibly, of R_θ). Since Head's original paper, several workers had proposed alternatives to, or refinements of, his hypotheses concerning the entrainment and shape-parameter relationships. It was felt, however, that these proposals had not led to any prediction method which showed an appreciable all-round improvement over Head's original method. Hence, in deriving the present method, Head's proposals were followed as closely as the requirements of internal consistency would allow (in Appendix B, one possible way of refining the semi-empirical basis of the method is discussed).

In the first place, his empirical correlation between C_E and H_1 was taken at face value. The expression

$$C_E = 0.0299(H_1 - 3.0)^{-0.6169} \quad (8)$$

which has been given by Thompson¹² as a fit to Head's graphical relationship was adopted. It differs marginally from the relation used in Ref. 2, which was drawn from a different source.

The empirical relation between H and H_1 derived by Head was not however used. Instead, a relationship between H and H_1 was derived by empirically distorting the curve of $H(H_1)$ obtained from a family of wake-like velocity profiles. If the wake function of Coles¹³ is approximated by $1 - \cos \pi y/\delta$ (as was done for example in Ref. 14), and we consider boundary layers in the limit of infinite Reynolds number where the logarithmic inner law provides only a slip velocity at the inner edge of this wake profile, the resulting Coles profile family gives the relation

$$H - 1 = H_1 - 2 \mp \sqrt{(H_1 - 2)^2 - 3}. \quad (9)^*$$

The form of this curve is qualitatively the same as those given by Thompson's⁴ profile family, notably in that it has a minimum in H_1 (at $H = 1 + \sqrt{3}$, $H_1 = 2 + \sqrt{3}$ from equation (9)). It is also a fairly good quantitative approximation both to Thompson's family at high R_θ and to experimental results.

If, however, the prediction method had been completed by the use of equation (9), it would have had an unnecessary shortcoming; calculations in constant-pressure flows would not have reproduced the variation of C_{f_0} and H_0 with R_θ given by equations (5) and (6), even if starting values were chosen to fit these equations. Therefore, the curve given by equation (9) was empirically deformed to produce a relation which, when used in conjunction with the entrainment formula of equation (8) and the skin friction law of equations (5) to (7), closely reproduced the zero pressure gradient behaviour specified in equations (5) and (6). As used during the calculation process this relation was written

$$H = 1 + 1.12(H_1 - 2 - \sqrt{(H_1 - 2)^2 - 3})^{0.915} \quad (10)$$

for attached flows. At the start of a calculation the preferred course was usually to specify H rather than H_1 ; to provide an initial value of H_1 for the calculation, therefore, the following inversion of equation (10) was needed:

$$H_1 = 2 + 1.5 \left(\frac{1.12}{H-1} \right)^{1/0.915} + 0.5 \left(\frac{H-1}{1.12} \right)^{1/0.915}. \quad (11)$$

In Fig. 3 the trajectory of H_0 against C_{f_0} obtained from a calculation in zero pressure gradient is compared with the initially assumed trajectory of equations (5) and (6). Also shown for interest is the trajectory obtained by applying Head's original method in zero pressure gradient, which gives a flat-plate value for G of 7.4 approximately. Clearly, the coupling of equations (5) to (7), (8) and (10) has succeeded in 'tying' the method to flat-plate behaviour throughout the range of Reynolds numbers of practical interest. Consequently, for flows with moderate pressure gradients which do not cause large departures from flat-plate conditions, the method for incompressible flow might be expected to remain fairly accurate at all Reynolds numbers.

2.4. Treatment of Wakes

After the basic method for attached boundary layers had been developed and tested, a simple modification was introduced to enable some estimate to be made of the development of aerofoil wakes.

Consider first the flow downstream of a symmetrical aerofoil at zero incidence. If the definitions of equation (1) are retained—so that thicknesses are defined by integrations across half the wake—the forward integration of equations (2) and (4) may be smoothly carried on from the aerofoil surface, past the trailing edge and into the wake. The only change in equations (2) and (4) is that C_f becomes zero everywhere downstream of the trailing edge. Whether or not the empirical formulae for C_E and H can still be employed is another question. However, since equation (10) was only slightly different from the family of wake profiles of equation (9), and

* The square root term is subtracted for attached boundary layers.

since it was desirable that both H and H_1 should be continuous through the trailing edge station, it was thought justified to retain equation (10) in the wake region. Accordingly, the only modification made to the method was to adjust the entrainment formula to take account of the more vigorous turbulent processes observed in far wakes.

In constant pressure wakes with small velocity defect it has been shown by similarity arguments that, when viscosity can be neglected, the shape-parameter will tend asymptotically to unity at a rate

$$\theta \frac{dH}{dx} = -A(H-1)^3 \quad (12)$$

where A is a constant. Measurements by Townsend⁵ far downstream of a circular cylinder indicate a value of 0.234 for A . If equation (10) is used to relate H and H_1 , to make equations (4) and (12) equivalent we thus write:

$$C_{EFW} = 0.435(H-1)^{0.907}. \quad (13)$$

Rather than have the method 'switch' from equation (8) to equation (13) on passing a trailing edge, which would have implied a physically unrealistic, discontinuous increase in C_E , it was arranged for C_E to increase asymptotically towards its far wake value C_{EFW} . Some measurements by Cook¹⁵ downstream of a symmetrical aerofoil were used to estimate how rapid the increase should be. Entrainment in the wake C_{EW} was defined as a weighted mean of the 'attached flow' value C_E given by equation (8) and the 'far wake' value C_{EFW} given by equation (13): viz.

$$C_{EW} = \gamma C_{EFW} + (1-\gamma)C_E. \quad (14)$$

From Cook's experiments, it appeared adequate to approximate the weighting function by

$$\gamma = 1 - \exp\left(\frac{x_{TE} - x}{5\delta_{TE}}\right) \quad (15)$$

where suffix TE denotes values at the trailing edge.

Thus, for a symmetrical aerofoil at zero lift, the boundary layer calculation for one surface could be extended into the wake by carrying on the integration of equations (2) and (4) with C_f set to zero and C_E set to C_{EW} , evaluated from equation (15) using equations (8), (13) and (14). Alternatively, the momentum and displacement thicknesses could be defined as integrals across the whole wake. In this case, starting at the trailing edge, values of θ and δ^* in the calculation would be twice as large, shape parameters would remain unchanged, the length scale in equation (15) would be $2.5\delta_{TE}$, and the first term on the right-hand side of equation (4) would be $2C_{EW}$, since account would now have to be taken of entrainment into both edges of the wake. Because of the symmetry, the two types of calculation would of course give identical results.

When boundary layers on the upper and lower surfaces do not have the same properties at the trailing edge, as will usually be the case if the external flow field is not completely symmetrical, either of the above approaches may be used provided some further degree of approximation is accepted. The most convenient course is usually to continue upper and lower surface calculations separately into the far wake, and then to obtain overall integral parameters at any station by adding together the appropriate upper and lower integrals. In so doing, the effect of any shear stress on the dividing streamline between the upper and lower parts of the wake is neglected. As this stress makes an equal and opposite contribution to the momentum integral equations for the two parts of the wake, its neglect may be expected to have only a second-order effect on overall parameters. The alternative course is to add together upper and lower thickness parameters at the trailing edge, and then perform the calculation for the total wake, treating it as if it were symmetrical. These two procedures give very similar results. In the limited comparisons with experiment that have been possible both procedures yield results which from an engineering standpoint are of quite acceptable accuracy.

3. The Method for Compressible Flows

3.1. Basic Equations

In compressible flow, the parameters which occur in the present method are defined as:

$$\begin{aligned}
 \text{displacement thickness} \quad & \delta^* = \int_0^\infty \left(1 - \frac{\rho u}{\rho_e u_e}\right) dy \\
 \text{momentum thickness} \quad & \theta = \int_0^\infty \frac{\rho u}{\rho_e u_e} \left(1 - \frac{u}{u_e}\right) dy \\
 \text{mass-flow thickness} \quad & \Delta = \int_0^\delta \frac{\rho u}{\rho_e u_e} dy \\
 & H = \delta^* / \theta \\
 \text{shape parameters} \quad & H_1 = \Delta / \theta \\
 & \bar{H} = \frac{1}{\theta} \int_0^\infty \frac{\rho}{\rho_e} \left(1 - \frac{u}{u_e}\right) dy \\
 \text{skin-friction coefficient} \quad & C_f = \frac{\tau_w}{\frac{1}{2} \rho_e u_e^2} \\
 \text{and entrainment coefficient} \quad & C_E = \frac{1}{r \rho_e u_e} \frac{d}{dx} \left(r \int_0^\infty \rho u dy \right) \\
 & = \frac{1}{r \rho_e u_e} \frac{d}{dx} (r \rho_e u_e \Delta).
 \end{aligned} \tag{16}$$

The momentum-integral equation in axisymmetric compressible flow may be written:

$$\begin{aligned}
 \frac{d\theta}{dx} &= \frac{C_f}{2} - (H+2) \frac{\theta}{u_e} \frac{du_e}{dx} - \frac{\theta}{\rho_e} \frac{d\rho_e}{dx} - \frac{\theta}{r} \frac{dr}{dx} \\
 &= \frac{C_f}{2} - (H+2 - M_e^2) \frac{\theta}{u_e} \frac{du_e}{dx} - \frac{\theta}{r} \frac{dr}{dx}
 \end{aligned} \tag{17}$$

where M is Mach number, and the definition of C_E , from equations (16), may be recast either as a rate equation for mass-flow thickness

$$\begin{aligned}
 \frac{d\Delta}{dx} &= C_E - \frac{\Delta}{u_e} \frac{du_e}{dx} - \frac{\Delta}{\rho_e} \frac{d\rho_e}{dx} - \frac{\Delta}{r} \frac{dr}{dx} \\
 &= C_E - (1 - M_e^2) \frac{\Delta}{u_e} \frac{du_e}{dx} - \frac{\Delta}{r} \frac{dr}{dx}
 \end{aligned} \tag{18}$$

or, combining this latter with equation (17), as a shape-parameter equation

$$\theta \frac{dH_1}{dx} = C_E - H_1 \left(\frac{C_f}{2} - (H+1) \frac{\theta}{u_e} \frac{du_e}{dx} \right). \tag{19}$$

It may be noted that in this form the terms in density and radius are absent, so that equation (19) is identical with the equation (4) for incompressible flow. And, as in incompressible flow, the three unknowns for which auxiliary relations are needed during the integration of equations (17) and (19) are C_f , C_E and H . These relations are given in the following sections.

3.2. Skin-Friction Relations

For compressible flow in zero pressure gradient, Spalding and Chi³ introduced scaling parameters (written here F_c and F_R) such that the scaled skin-friction coefficient $F_c C_f$ and the scaled Reynolds number $F_R R_\theta$

satisfied the $C_f(R_\theta)$ relation which they had proposed for incompressible flow. Thus, the present analytic approximation to their relation, equation (5), could be written

$$F_c C_{f_0} = \frac{0.012}{\log_{10} F_R R_\theta - 0.64} - 0.00093. \quad (20)$$

To evaluate F_c and F_R it was convenient to introduce the temperature ratios

$$R = \frac{T_r}{T_e} = 1 + r \frac{\gamma - 1}{2} M_e^2$$

and (21)

$$W = \frac{T_w}{T_e} = \frac{T_w}{T_{oe}} \left(1 + \frac{\gamma - 1}{2} M_e^2 \right)$$

where r was the temperature recovery factor, and suffixes r , w and oe denoted recovery, wall, and free stream stagnation temperatures respectively. The empirical expressions which Spalding and Chi put forward for the scaling factors in their skin-friction relation could then be written

$$F_c = \frac{R - 1}{\left[\arctan \left(\frac{R - W}{2\sqrt{W(R - 1)}} \right) - \arctan \left(\frac{2 - R - W}{2\sqrt{R - 1}} \right) \right]^2}$$

and (22)

$$F_R = R^{0.772} W^{-1.474}.$$

To incorporate this flat-plate skin-friction law into a more general relation, applicable to flows with pressure gradients, it was necessary to introduce a dependence on the shape of the velocity profile. For this purpose it was assumed that in compressible flow the 'transformed' shape parameter \bar{H} played an equivalent role, in characterising the shape of the velocity profile, to that played by the conventional shape parameter H in incompressible flow. Thus, the value of \bar{H} in zero pressure gradient was given by writing equation (6)

$$\bar{H}_0 = 1 / \left(1 - 6.8 \sqrt{\frac{C_{f_0}}{2}} \right) \quad (23)$$

and skin friction in general compressible flows was obtained by writing equation (7):

$$\left(\frac{C_f}{C_{f_0}} + 0.5 \right) \left(\frac{\bar{H}}{\bar{H}_0} - 0.4 \right) = 0.9. \quad (24)$$

The use of these two equations undoubtedly involved some sacrifice in accuracy for the sake of simplicity. Equation (23) was probably the most suspect; recent experimental evidence of Winter and Gaudet¹⁰ suggests that it introduced a systematic error increasing with Mach number such that, at a Mach number of 2.8, \bar{H}_0 would be underestimated by about 3 per cent. On the other hand, this equation was consistent with the adopted entrainment and shape-parameter relationships; given the latter it was, in effect, a direct result of the need to reproduce satisfactorily the skin friction and momentum thickness distributions which had been specified analytically for flows with zero pressure gradient.

In Fig. 4 the skin-friction law as a whole, equations (20) to (24), is compared with some experimental results obtained in flow at $M \sim 2$, at virtually constant pressure, downstream of a region of shock and boundary-layer interaction (*see* Ref. 2). Skin friction was determined from Preston tube readings and \bar{H} from pitot traverses across the boundary layer. This comparison broadly confirms the skin-friction law, particularly in respect of the variation of C_f with \bar{H} given by equation (24). At the same time there is some evidence to support the reservation expressed in the previous paragraph, in that the results are consistent with a slight underestimation of \bar{H}_0 by equation (23).

3.3. Other Auxiliary Relations

To complete the method, relations were needed for \bar{H} , H and C_E ; these were obtained by making the simplest assumptions consistent with our (very limited) understanding of the structure of compressible, turbulent flow.

In the preceding section we introduced the assumption that, to characterise the shape of the velocity profile, the 'transformed' shape parameter \bar{H} might be regarded as the equivalent in compressible flow of the parameter H at low speeds. The arguments that led to this assumption (see Ref. 2) suggested, at the same time, that the parameter H_1 provided an indication of the character of the velocity profile which applied equally well to both compressible and incompressible flows. Thus, by substituting \bar{H} for H but leaving H_1 unchanged, equation (10) was written

$$\bar{H} = 1 + 1.12(H_1 - 2 - \sqrt{(H_1 - 2)^2 - 3})^{0.915} \quad (25)$$

and its inversion, equation (11), became

$$H_1 = 2 + 1.5 \left(\frac{1.12}{\bar{H} - 1} \right)^{1/0.915} + 0.5 \left(\frac{\bar{H} - 1}{1.12} \right)^{1/0.915}. \quad (26)$$

In Fig. 5 this relation is compared with the same set of experimental results, obtained at $M \sim 2$, that was used in Fig. 4 to check the skin-friction relation. Agreement is satisfactory in that it is no worse—indeed it is somewhat better—than the agreement found by Head, for incompressible flow, between his graphical relation and the rather scattered experimental results from which it was derived.

To evaluate the shape parameter $H (= \delta^*/\theta)$ from \bar{H} , it was assumed that static temperature through the boundary layer could be adequately represented by the familiar quadratic expression

$$T = T_w + (T_r - T_w) \frac{u}{u_e} + (T_e - T_r) \left(\frac{u}{u_e} \right)^2,$$

from which it followed that

$$H = \frac{T_w}{T_e} \bar{H} + \frac{T_r}{T_e} - 1. \quad (27)$$

This is the same relation that was used in the second method of Ref. 2, where its limitations are briefly discussed.

Finally, it was assumed that the relation between C_E and H_1 which had been adopted for incompressible flow could be carried over unchanged into compressible flow

$$C_E = 0.0299(H_1 - 3.0)^{-0.6169}. \quad (28)$$

This assumption led to an appreciably simpler and more tractable method than was obtained in Ref. 2, where C_E was assumed to depend on a 'kinematic' shape parameter of the boundary layer. Estimates of C_E from equation (28) were lower than those obtained from the earlier assumption. Nevertheless, as Fig. 6 shows, the difference between the two assumptions was not large compared with the uncertainties associated with the experimental data. In zero pressure gradient, if H_1 varies slowly with x , its value should be very nearly $2C_E/C_f$ (from equation (19)). In Fig. 6, values of H_1 measured in zero pressure gradient are compared with the variation of $2C_E/C_f$, according to various hypotheses, at a constant length Reynolds number. An earlier version of the figure, and a fuller discussion, were given in Ref. 2; the two lines added since then, a relation adopted by Bradshaw and Ferriss¹⁶ and the one implied by the present equation (28), are seen to be almost identical. In the light of the previous discussion² of the experimental data in Fig. 6, the agreement with the line given by equation (28) is considered ample justification for the adoption of this relation unaltered in compressible flows.

3.4. Summary of Method

In compressible flow, development of a turbulent boundary layer may be predicted in terms of the momentum thickness θ and shape parameter H_1 , by simultaneous forward integration of the momentum integral equation, equation (17), and the entrainment-based shape parameter equation, equation (19). The other unknowns needed in these equations are evaluated as follows:

\bar{H} from equation (25), H from equation (27), C_E from equation (28) and C_f from equations (20) to (24). If some parameter other than H_1 is used to specify the initial shape of the velocity profile (e.g. C_f or H), the corresponding value of \bar{H} may be determined from whichever of the above relations is appropriate, and H_1 then obtained from equation (26). The choice of a relation between viscosity and temperature, needed for the evaluation of R_θ , is left to the discretion of the user; as programmed at R.A.E., the method used Sutherland's relation.

In adiabatic flows with significant pressure gradients, where accurate evaluation of H is important, the recovery factor is probably best taken as unity so that $T_w/T_e = T_r/T_e = T_{oe}/T_e$. This assumption has been the one most commonly employed at R.A.E. The integration of equations (17) and (19) on a computer is quick and straightforward using a standard procedure of, for example, the Runge-Kutta type. Programmed in EMA, a typical calculation over a complete aerofoil and wake to a point two chord lengths downstream of the trailing edge occupied roughly five seconds of central processor time on an ICL 1907 computer.

4. Comparisons with Experiment

Thompson¹⁷ and, later, Kline, *et al.*,⁶ have made extensive comparisons between the predictions of Head's original method and experiment for incompressible flows. At the Stanford Conference⁶ Head's method was placed in the second division, emerging as a method which gave reasonably accurate predictions in most circumstances but which in certain cases, notably 'equilibrium' and 'relaxing' flows, was clearly not as accurate as those six more recent and sophisticated methods which were placed in the first division. In extending the method to compressible flow the most we can reasonably hope is that, in the process, its shortcomings have been neither added to nor aggravated appreciably.

Fig. 7 compares measured values of shape parameter with predictions by Head's original method and by the present method for three incompressible flows which were mandatory cases at the Stanford Conference. The small but significant differences between the two methods (not attributable to computing differences, since formally identical computer programs and input data were used for the two sets of calculations) are typical of their relative performance over the whole range of Stanford cases. In some cases the original method is the more accurate, in others the present method; on balance, neither emerges with any clear superiority.

Of the three cases shown, the Shubauer and Klebanoff flow is of the 'aerofoil' type in which Head's method generally works well—the underestimation of H towards the rear of the model in this flow is typical of the 'first division' methods also, and is due in some part to flow convergence in the experiment. The other two flows, Clauser's second equilibrium flow and Bradshaw's relaxing flow, illustrate the two situations in which Head's method is at its least accurate.

Fig. 8 shows predictions by the present method of boundary layer and wake development, this time in terms of momentum and displacement thickness, for a two-dimensional lifting aerofoil at moderately high subsonic speed. The experimental measurements by Cook¹⁸ are seen to be predicted to fairly good engineering accuracy and, in particular, the sharp peak in momentum and displacement thickness at the trailing edge is well approximated. The method has been compared with a number of such subsonic flows and, on the basis of the generally good agreement found, is now being used iteratively¹⁹, in conjunction with a method for the outer inviscid flow, as a prediction method for viscous flows over aerofoils.

Fig. 9 shows predictions of shape parameter, momentum thickness and skin-friction coefficient for a waisted body of revolution tested at subsonic and supersonic speeds by Winter, Rotta and Smith²⁰. From the two examples shown, it is seen that the variation of all the flow parameters, notably the large increase in momentum thickness and the reduction in skin friction at the waist, followed by a decrease in momentum thickness and appreciable increase in skin friction over the flared rear of the body, is fairly well predicted at $M_\infty = 0.6$, Fig. 9a. However, at $M = 2.0$ (Fig. 9b) the increase in skin friction over the rear of the body is considerably underestimated; this shortfall in C_f is consistent with, and may be attributed to, the overestimation of H in this region. It may be noted that other published predictions (e.g. Refs. 16, 21) of these flows have shown a similar underestimation of the change in skin friction over the rear of the body at supersonic speeds.

Finally, in Fig. 10, a comparison is made between the present method and the two earlier applications of Head's method in compressible flow developed by the author². The experimental results are for a flow at $M = 2.0$ downstream of a region of separation induced by an incident-reflecting shock of 8 degrees deflection.

As might have been expected, the present method lies between the two earlier methods, tending towards the preferred one of these two rather than towards that involving a transformation. This relaxing type of flow is of course one in which good agreement is not expected. However, for reasons given when making previous comparisons with this flow², it is not easy to assess from the evidence at low speeds how much in error a realistic extension of Head's method to compressible flows should be in this particular situation. Hence it is difficult to say from Fig. 10 which method is potentially the most accurate when applied to less severely disturbed supersonic flows.

5. Conclusions

This Report provides a record of the version of Head's turbulent boundary-layer method that has been in use in R.A.E. and other centres since 1967. The method has been used for boundary layers and wakes in compressible flows with zero heat transfer (in Appendix A an untried extension of the method to flows with heat transfer is given).

The present version has been derived by replacing the empirical relations originally proposed by Head by closely similar ones which explicitly 'tie' the method to the well-documented reference case of the boundary layer in zero pressure gradient. The empirical correlation of Spalding and Chi, for flat-plate boundary layers in compressible flow, is then used to tie the method to the flat plate for the full Mach-number range—up to $M = 4.5$, say, for which reasonably reliable skin-friction data are available.

Wake flows are predicted by dropping the skin friction term from the equations and introducing a modified empirical relation for entrainment coefficient which tends, far downstream, towards that observed by Townsend in the far wake of a cylinder.

Comparisons with experiments illustrate the accuracy of the method for engineering predictions over a wide range of flow conditions. At the same time, they show the order of the errors—significant but not gross—which arise when the method is used in particularly testing conditions. Although it is clearly not as accurate or as versatile as the most sophisticated of recent methods, the combination of simplicity, speed of computation and general reliability which it provides makes this version of Head's method a tool which still has many useful applications in the field of aerodynamics.

LIST OF SYMBOLS

C_E	Entrainment coefficient (equations (1), (16))
C_f, C_{f_0}	Skin-friction coefficient (equations (1), (16)), flat-plate skin-friction coefficient
C_p	Specific heat at constant pressure
F_c, F_R	Factors on C_f and R_θ in compressible skin-friction formulae (equations (22), (B-10))
H, \bar{H}, H_1, H_2	Shape parameters (equations (1), (16), (A-2))
H_0, \bar{H}_0	Shape parameters in zero pressure gradient
M	Mach number
Pr	Prandtl number
q_w	Heat-transfer rate to the wall
Q	Non-dimensional wall heat-transfer rate (equation (A-1))
r	Body radius
r	Temperature-recovery factor
R, W	Temperature ratios in Spalding and Chi formula (equation (21))
R_θ	Reynolds number based on momentum thickness
T, T_0	Static temperature, stagnation temperature
u, v	Velocity components in x and y directions
u_τ	Friction velocity ($=\sqrt{\tau_w/\rho_w}$)
x, y	Coordinates along and normal to surface
ρ	Density
$\delta, \delta^*, \Delta, \theta$	Boundary-layer thickness, displacement thickness, mass-flow thickness, momentum thickness (equations (1), (16))
τ	Shear stress
γ	Weighting function (equation (15))
<i>Subscripts</i>	
e	Denotes conditions at edge of boundary layer
r	Denotes conditions at wall in adiabatic flow
s	Denotes conditions at edge of 'thermal sublayer'
w	Denotes conditions at wall
TE	Denotes conditions at the trailing edge
W, FW	Denotes conditions in the wake, and far wake

REFERENCES

- | <i>No.</i> | <i>Author(s)</i> | <i>Title, etc.</i> |
|------------|------------------------------------|--|
| 1 | M. R. Head | Entrainment in the turbulent boundary layer.
A.R.C. R. & M. 3152 (1958). |
| 2 | J. E. Green | The prediction of turbulent boundary layer development in compressible flow.
<i>J. Fluid Mech.</i> , 31, 753-778 (1968). |
| 3 | D. B. Spalding and S. W. Chi | The drag of a compressible turbulent boundary layer on a smooth flat plate with and without heat transfer.
<i>J. Fluid Mech.</i> , 18, 117-143 (1964). |
| 4 | B. G. J. Thompson | A new two-parameter family of mean velocity profiles for incompressible turbulent boundary layers on smooth walls.
A.R.C. R. & M. 3463 (1965). |
| 5 | A. A. Townsend | <i>The structure of turbulent shear flow.</i>
Cambridge University Press (1956). |
| 6 | S. J. Kline, <i>et al.</i> | Computation of turbulent boundary layers—proceedings of the 1968 A.F.O.S.R.-I.F.P.-Stanford Conference (1968). |
| 7 | H. Ludwig and W. Tillman | Untersuchungen über die Wandschubspannung in turbulenten Reibungsschichten.
<i>Ing. Arch.</i> , 17, 288-299 (1949).
N.A.C.A. T.M. 1285 (English translation) (1950). |
| 8 | F. H. Clauser | Turbulent boundary layers in adverse pressure gradients.
<i>J. Aeronaut. Sci.</i> , 21, 91-108 (1954). |
| 9 | D. E. Coles | The turbulent boundary layer in a compressible fluid.
U.S.A.F. Project Rand Rept R-403-PR (1962). |
| 10 | K. G. Winter and L. Gaudet | Turbulent boundary layer studies at high Reynolds numbers at Mach numbers between 0.2 and 2.8.
A.R.C. R. & M. 3712 (1970). |
| 11 | J. F. Nash and A. G. J. Macdonald | A turbulent skin friction law for use at subsonic and transonic speeds.
A.R.C. C.P. 948 (1966). |
| 12 | B. G. J. Thompson | The calculation of shape parameter development in incompressible turbulent boundary layers with or without transpiration.
AGARDograph 97, 159-190 (1965). |
| 13 | D. E. Coles | The law of the wake in the turbulent boundary layer.
<i>J. Fluid Mech.</i> , 1, 191-226 (1956). |

REFERENCES (continued)

- 14 J. E. Green Two-dimensional turbulent reattachment as a boundary layer problem.
A.G.A.R.D. C.P. 4, 393-428.
R.A.E. Technical Report 66059 (1966).
- 15 T. A. Cook R.A.E. unpublished.
- 16 P. Bradshaw and D. H. Ferriss Calculation of boundary-layer development using the turbulent energy equation: compressible flow on adiabatic walls.
J. Fluid Mech., 46, 83-110 (1971).
- 17 B. G. J. Thompson A critical review of existing methods of calculating the turbulent boundary layer.
A.R.C. R. & M. 3447 (1964).
- 18 T. A. Cook Measurements of the boundary layer and wake of two aerofoil sections at high Reynolds number and high subsonic Mach numbers.
A.R.C. R. & M. 3722 (1971).
- 19 M. C. P. Firmin Calculation of the pressure distribution, lift and drag on aerofoils at subcritical conditions. Part 1, Interim method.
R.A.E. Technical Report 72235 (1972).
- 20 K. G. Winter, J. C. Rotta and K. G. Smith Studies of the turbulent boundary layer on a waisted body of revolution in subsonic and supersonic flow.
A.R.C. R. & M. 3633 (1968).
- 21 H. McDonald An assessment of certain procedures for computing the compressible turbulent boundary layer development.
N.A.S.A. S.P. 216, Paper No. 6 (1968).
- 22 J. C. Rotta Heat transfer and temperature distribution in turbulent boundary layers at supersonic and hypersonic flow.
AGARDograph 97, 35-63 (1965).
- 23 J. P. Johnson On the three-dimensional turbulent boundary layer generated by secondary flow.
Trans. ASME Ser. D, 82 (1960).
- 24 J. E. Green, D. J. Weeks and J. W. F. Brooman Prediction of turbulent boundary layers and wakes in compressible flow by a lag-entrainment method.
R.A.E. Tech. Report 72231 (1973).
To be published as an R. & M.
- 25 P. Bradshaw, D. H. Ferriss and N. P. Attwell Calculation of turbulent boundary layer development using the turbulent energy equation.
J. Fluid Mech., 28, 593-616 (1967).

REFERENCES (concluded)

- 26 J. F. Nash Turbulent boundary layer behaviour and the auxiliary equation. AGARDograph 97, 245-279 (1965).
- 27 J. C. Rotta Turbulent boundary layers in incompressible flow. Prog. Aeronaut. Sci., Vol. 2, 1-219, Pergamon Press (1962).
- 28 W. J. Sumner and J. R. Shanbrook Entrainment theory for compressible turbulent boundary layers on adiabatic walls. *A.I.A.A. Journal*, 9, 2, 330-332 (1971).
- 29 J. E. Green, D. J. Weeks and J. W. F. Brooman An integral prediction method for turbulent boundary layers with heat transfer based on a simple polar of temperature against velocity. R.A.E. unpublished paper presented at Euromech 43 Colloquium on 'Heat transfer in turbulent boundary layers with variable fluid properties'. Göttingen, May 1973.
- 30 V. K. Verma A method of calculation for two-dimensional and axisymmetric boundary layers. University of Cambridge, Department of Engineering CUED/A Aero/TR3 1971.

APPENDIX A

Application to Compressible Flows with Heat Transfer

In this Appendix a simple, tentative extension of the method to flows with heat transfer is put forward. It has not been tested against experiment, and is put forward here only because (1) integral methods applicable to flows with heat transfer are not numerous and (2) the basic framework of the method is thought capable of being adapted to keep abreast of advances in understanding of the physical mechanisms underlying the turbulent heat-transfer process.

For flows with heat transfer, the boundary-layer development is calculated by forward integration of *three* simultaneous ordinary differential equations, the momentum-integral equation, the entrainment equation and the total-energy equation

$$\frac{d}{dx}(r\rho_e u_e H_2 \theta) = \frac{r q_w}{C_p T_{oe}},$$

which can be combined with the momentum integral equation to give

$$\theta \frac{dH_2}{dx} = Q - H_2 \left[\frac{C_f}{2} - \theta(H+1) \frac{1}{u_e} \frac{du_e}{dx} \right], \quad (\text{A-1})$$

where $Q = q_w / \rho_e u_e C_p T_{oe}$ is the non-dimensional rate of heat transfer to the wall and H_2 is the total enthalpy defect shape parameter, given by

$$H_2 = \frac{1}{\theta} \int_0^\infty \frac{\rho u}{\rho_e u_e} \left(1 - \frac{T_0}{T_{oe}} \right) dy \quad (\text{A-2})$$

for a gas with C_p , the specific heat at constant pressure, constant.

The empiricism in the method is introduced through the assumed family of temperature profiles. Two different forms of the Crocco integral (both cited by Rotta²²) are adopted, one matched to the boundary condition at the wall, the other matched to the integrated total enthalpy defect in the outer part of the boundary layer.

The latter is simply the linear relation

$$1 - \frac{T_0}{T_{oe}} = H_2 \left(1 - \frac{u}{u_e} \right), \quad (\text{A-3})$$

which is one way of writing Crocco's solution (for flow at constant pressure and wall temperature with a Prandtl number of unity) and is the limiting form at high Reynolds numbers for flows in which the temperature-velocity polar is linear outside a thin layer close to the wall (the contribution to the boundary layer defect integrals from the latter being neglected).

The wall-region version of the Crocco integral is

$$\frac{T_0}{T_{oe}} = \frac{T_w}{T_{oe}} + 2Pr \frac{Q}{c_f} \left(\frac{u}{u_e} \right) + (1-Pr) \left(1 - \frac{T_e}{T_{oe}} \right) \left(\frac{u}{u_e} \right)^2 \quad (\text{A-4})$$

which applies to the region in which shear stress and Prandtl number, Pr , are effectively constant and convection terms are negligible.

If these two temperature distributions intersect at the edge of some thermal sublayer denoted by suffix s , the heat transfer coefficient may be obtained by combining them to give

$$2Pr \frac{Q}{c_f} \left(\frac{u}{u_e} \right)_s = 1 - \frac{T_w}{T_{oe}} - H_2 \left(1 - \left(\frac{u}{u_e} \right)_s \right) - (1-Pr) \left(1 - \frac{T_e}{T_{oe}} \right) \left(\frac{u}{u_e} \right)_s^2, \quad (\text{A-5})$$

where it is now necessary to adopt some empirical criterion for determining the edge of the sublayer.

There are strong parallels between this representation of the temperature-velocity polar and Johnson's²³ triangular representation of the crossflow velocity polars in three-dimensional boundary layers. Indeed,

for want of an exhaustive search and correlation of the available experimental data, we postulate an equivalence between the junction points between the inner and outer parts of the crossflow and temperature polars, and suggest here the adoption of Johnson's proposal that this junction point occurs at a constant value of $(u/u_\tau)_s = 14$ (Johnson actually took it as $10\sqrt{2}$, and we shall follow him).

Assuming that this argument can be carried over to compressible flow, provided u_τ is based on density at the wall, we have

$$\begin{aligned} \left(\frac{u}{u_e}\right)_s &= 10\sqrt{2}\frac{u_\tau}{u_e} \\ &= 10\sqrt{\frac{T_w}{T_e}C_f} \end{aligned} \quad (\text{A-6})$$

That this model of the flow is plausible may be seen by considering equation (A-5) for the case of an adiabatic wall ($Q = H_2 = 0$), when the conventional recovery factor r is given as

$$r = 1 - 100\frac{T_w}{T_e}C_f(1 - Pr). \quad (\text{A-7})$$

For $(T_w/T_e)C_f = 4 \times 10^{-3}$, a value typical of available turbulent boundary layer results in supersonic flow, and with $Pr = 0.72$, we find $r = 0.888$, which is again typical of available data on turbulent boundary layers in supersonic flow.

In Fig. 11 some possible polars are sketched, together with the corresponding velocity profile. This figure illustrates the reasonableness of the assumption that the outer, linear part of the polar can be taken to apply across the whole boundary layer for the purpose of evaluating integral quantities. The cases sketched are: adiabatic flow ($T_0 = T_{oe}$ over the outer part of the layer); the cooled flat plate, for which Reynolds analogy holds approximately and $\partial T_0/\partial u = \text{constant}$ over the outer part of the layer $= \partial T_0/\partial u_{\text{wall}}$; a typical cooled nozzle wall, on which the driving temperature difference decreases with distance downstream of the throat and a more concave upwards polar is found than on a flat plate; and a flow in which locally $T_w = T_{oe}$, but in which the boundary layer carries with it the result of passage over a heated surface somewhere upstream, with the result that there now is heat transfer from the boundary layer back to the wall. All these illustrations are of course schematic and conjectural.

To complete the method we assume:

- (1) that the skin-friction relation of equations (20) to (24) can be used unaltered;
- (2) that Head's entrainment relation, equation (28), can be used unaltered;
- (3) that the \bar{H}/H_1 relations of equations (25) and (26) can be used unaltered; but that
- (4) the relation for the conventional shape parameter H , equation (27), derived from the widely used quadratic equation for temperature, must be replaced by an equation based on the temperature-velocity relation of equations (A-3) and (A-4). For simplicity, the contribution from the wall region is neglected in deriving this relation. Thus, assuming equation (A-3) to apply across the whole boundary layer, it is not difficult to show that

$$H = \frac{T_{oe}}{T_e}(\bar{H} + 1 - H_2\bar{H}) - 1. \quad (\text{A-8})$$

Summary

The boundary layer in compressible flow with heat transfer is specified by three independent integral quantities, θ , H_1 and H_2 , and its development is calculated by the simultaneous forward integration of equations (17), (19) and (A-1). The unknowns in these equations are determined as follows: \bar{H} from equation (25), C_f from equations (20) to (24), H from equation (A-8), C_E from equation (28), Q or T_w/T_{oe} , whichever is unspecified, from equations (A-5) and (A-6).

The principal weakness of the method as specified here is the untried nature of the assumed temperature-velocity polar and, in particular, the simple criterion for determining the edge of the supposed thermal sublayer. Its principal virtue is that it treats arguably the three most important conservation equations for flows with heat transfer in such a way that large errors in prediction seem unlikely to be sustained over extended

lengths of flow. Clearly, the method needs testing, and, possibly, developing. It is presented here in its raw state on the chance that someone might find it sufficiently interesting to pursue further.

Postscript

Since this report was first written, the above method has been developed further²⁹. On substitution for $(u/u_e)_s$ from equation (A-6), (A-5) may be written

$$2B \frac{Q}{C_f} \frac{u_\tau}{u_e} = 1 - \frac{T_w}{T_{oe}} - H_2 \left(1 - A \frac{u_\tau}{u_e} \right) - C \left(1 - \frac{T_e}{T_{oe}} \right) \left(\frac{u_\tau}{u_e} \right)^2, \quad (\text{A-9})$$

where

$$\frac{u_\tau}{u_e} = \sqrt{\frac{T_w}{T_e} \frac{C_f}{2}}$$

and the constants A , B and C can be derived from (A-5) and (A-6) as simple functions of Pr and $(u/u_\tau)_s$.

The crucial step taken in the further development of the method has been to discard the interrelationship between A , B and C that follows from (A-5) and (A-6) and, instead, to treat them as independent empirical constants. Values for them have been derived by close matching of the predictions of the method to: (i) experimentally observed values of recovery factor in adiabatic, supersonic flow at constant pressure; (ii) the von Karman expression for Reynolds analogy factor in constant pressure flow over an isothermal wall ($2St/C_f = (1 - 2.77 u_\tau/u_e)^{-1}$, for a Prandtl number of 0.72); (iii) the heat transfer distribution predicted by a finite-difference method³⁰ for flow at constant pressure over a wall which is isothermal except for a single sinusoidal 'bump' in temperature. The resulting values for the constants are:

$$A = 17,$$

$$B = 14$$

$$\text{and } C = 55$$

$$(\text{A-10})$$

Predictions of heat transfer using the method of this appendix, and equations (A-9) and (A-10) rather than (A-5) and (A-6), have been made²⁹ only with a later version of the entrainment method²⁴, the 'lag-entrainment' method derived from the turbulent energy method of Bradshaw *et al.*²⁵. Agreement with a range of experimental data, mostly at laboratory Reynolds numbers ($R_\theta \sim 10^4$), is good: full details will be published in the near future.

APPENDIX B

Some Variations on the Basic Method

B.1. An 'Equilibrium' Entrainment Method

The method described in the body of this Report follows Head's original method fairly closely; in particular it incorporates without change the empirical relation which Head proposed between entrainment coefficient and the shape parameter H_1 . As a result the method performs similarly to Head's original method, giving fairly accurate predictions in pressure distributions typical of aerofoils but appreciably overestimating shape parameter in the 'equilibrium' flows studied by Clauser¹⁸.

Here, details are given of an entrainment method which works well in equilibrium flows, but which tends slightly to underestimate the trend towards separation in flows with adverse pressure gradients which increase in severity with streamwise distance. The method is a by-product of a lag-entrainment method²⁴ derived as an integral counterpart to the turbulent-kinetic-energy method of Bradshaw, *et al.*²⁵ Since it is tied to equilibrium flows, it has characteristics similar to a conventional mixing-length or eddy-viscosity method, and an indication of its probable accuracy may be obtained from the performance of methods of these two types at the Stanford Conference⁶.

For incompressible flow, the method is built around the equilibrium locus

$$\frac{H-1}{H} = 6.55 \sqrt{\frac{C_f}{2} - 0.8 \frac{\delta^*}{u_e} \frac{du_e}{dx}}, \quad (\text{B-1})$$

which lies very close to that proposed by Nash²⁶ but is a little more convenient algebraically. Equilibrium flows which follow this locus are assumed to be flows with constant H (consistent with Rotta's²⁷ strict definition), and a unique relation between H_1 and H is assumed. Then, from equation (4), in equilibrium flows

$$\theta \frac{dH_1}{dx} = 0 = C_E - H_1 \left(\frac{C_f}{2} - (H+1) \frac{\theta}{u_e} \frac{du_e}{dx} \right). \quad (\text{B-2})$$

Writing equation (B-1)

$$-\left(\frac{\theta}{u_e} \frac{du_e}{dx} \right)_{eq} = \frac{1.25}{H} \left(\left(\frac{H-1}{6.55H} \right)^2 - \frac{C_f}{2} \right) \quad (\text{B-3})$$

we have, from (B-2) and (B-3)

$$C_E = H_1 \left[\frac{C_f}{2} + 1.25 \frac{(H+1)}{H} \left(\left(\frac{H-1}{6.55H} \right)^2 - \frac{C_f}{2} \right) \right]. \quad (\text{B-4})$$

There is no reason why this entrainment relation should not be used with the shape parameter relation of equations (10) and (11). Formulated in this above way, the method is relatively insensitive to the particular $H-H_1$ relationship used except when the boundary layer is close to separation. In fact, the 'lag entrainment' method from which it is derived incorporates a slightly different relation,

$$H_1 = 3.15 + \frac{1.72}{H-1} - 0.01(H-1)^2 \quad (\text{B-5})$$

which has the merit of being simpler than equations (10) and (11), is thought to approximate boundary-layer behaviour in a sudden deceleration more accurately and, being monotonic for all $H > 1$, enables equations (2) and (4) to be integrated smoothly forward beyond separation without the method 'blowing up'. With this relation, it is convenient to take H rather than H_1 as the independent variable, with dH/dx obtained by multiplying equation (4) by $dH/dH_1(H)$.

For consistency with the equilibrium locus (B-1) the method should incorporate the skin-friction relation, derived from that of Winter and Gaudet¹⁰, described in the second part of this Appendix.

In compressible flow, it is assumed that the shape parameter relation equation (13) applies unchanged to H_1 and \bar{H} , and entrainment at equilibrium is defined by exactly the same equation, (B-2), as in incompressible flow. However, in compressible flow the equilibrium locus alters slightly. On an empirical basis, it has been suggested²⁴ that this be now written

$$\frac{\bar{H}-1}{\bar{H}} = 6.55 \sqrt{\left(\frac{C_f}{2} - 0.8H \frac{\theta}{u_e} \frac{du_e}{dx}\right) \left(1 + \frac{M_e^2}{25}\right)}, \quad (\text{B-6})$$

whence entrainment is given as:

$$C_E = H_1 \left[\frac{C_f}{2} + 1.25 \frac{(H+1)}{H} \left\{ \frac{1}{1+0.04M_e^2} \left(\frac{\bar{H}-1}{6.55\bar{H}} \right)^2 - \frac{C_f}{2} \right\} \right]. \quad (\text{B-7})$$

B.2. A Skin-Friction Relation Based on the Flat-Plate Relation of Winter and Gaudet

In the later 'lag entrainment'²⁴ method from which the above has been derived, the skin-friction relation has been tied to the flat-plate relation of Winter and Gaudet¹⁰ rather than that of Spalding and Chi³.

Equation (24) is still used unchanged,

$$\left(\frac{C_f}{C_{f_0}} + 0.5\right) \left(\frac{\bar{H}}{\bar{H}_0} - 0.4\right) = 0.9, \quad (\text{B-8})$$

but now we replace equation (20) by

$$F_c C_{f_0} = \frac{0.01013}{\log_{10} F_R R_\theta - 1.02} - 0.00075, \quad (\text{B-9})$$

equations (22) by

$$\left. \begin{aligned} F_c &= (1 + 0.2M_e^2)^{\frac{1}{2}} \\ F_R &= 1 + 0.056M_e^2 \end{aligned} \right\}, \quad (\text{B-10})$$

and equation (23) by

$$\bar{H}_0 = 1 / \left(1 - 6.55 \sqrt{\frac{C_{f_0}}{2} \left(1 + \frac{M_e^2}{25} \right)} \right). \quad (\text{B-11})$$

These relations are of course limited to adiabatic flow. If the method of this Appendix were combined with that of Appendix A to predict flows with heat transfer it would be necessary to revert to the formulae of Spalding and Chi, equations (20) to (22). However, for consistency with equation (B-4) it would in this case still be necessary to replace equation (23) by equation (B-11).

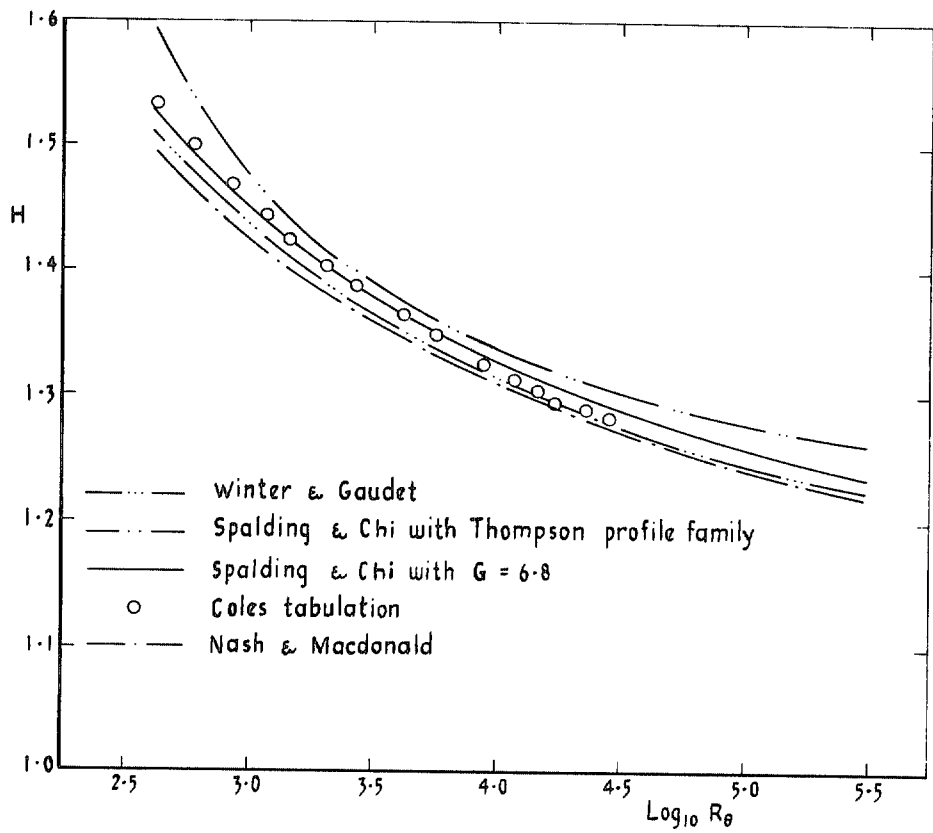


FIG. 1. Variation of shape parameter with Reynolds number in incompressible flow at constant pressure.

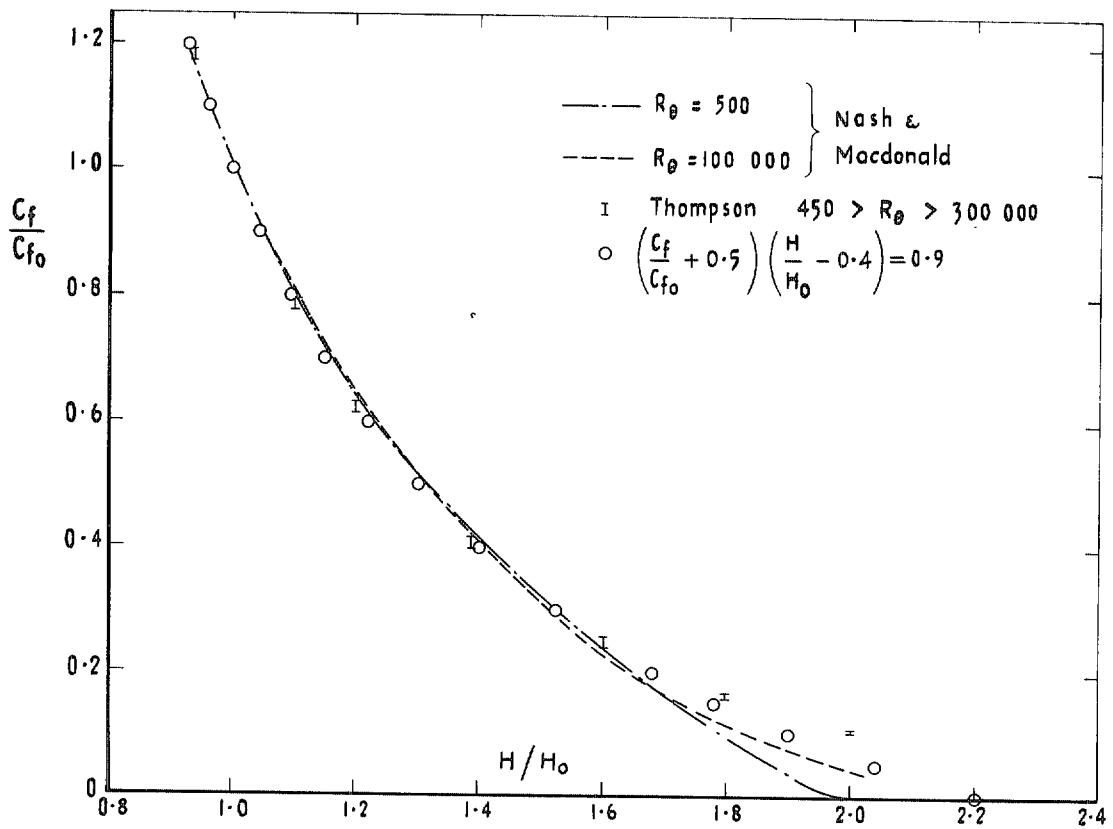


FIG. 2. Variation of skin-friction coefficient with shape parameter at constant R_θ in incompressible flow.

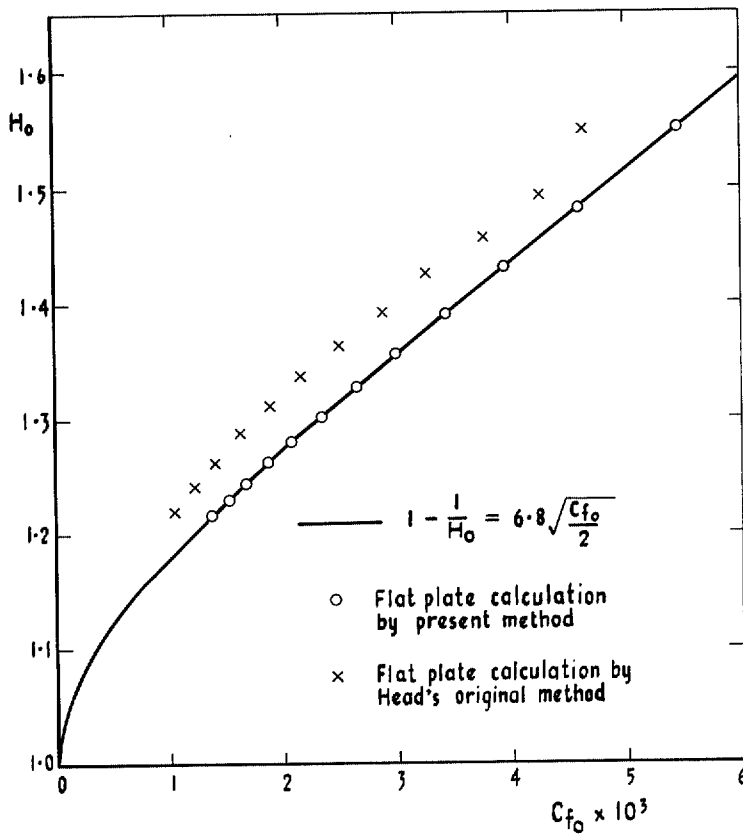


FIG. 3. Variation of shape parameter with skin-friction coefficient in incompressible flow at constant pressure.

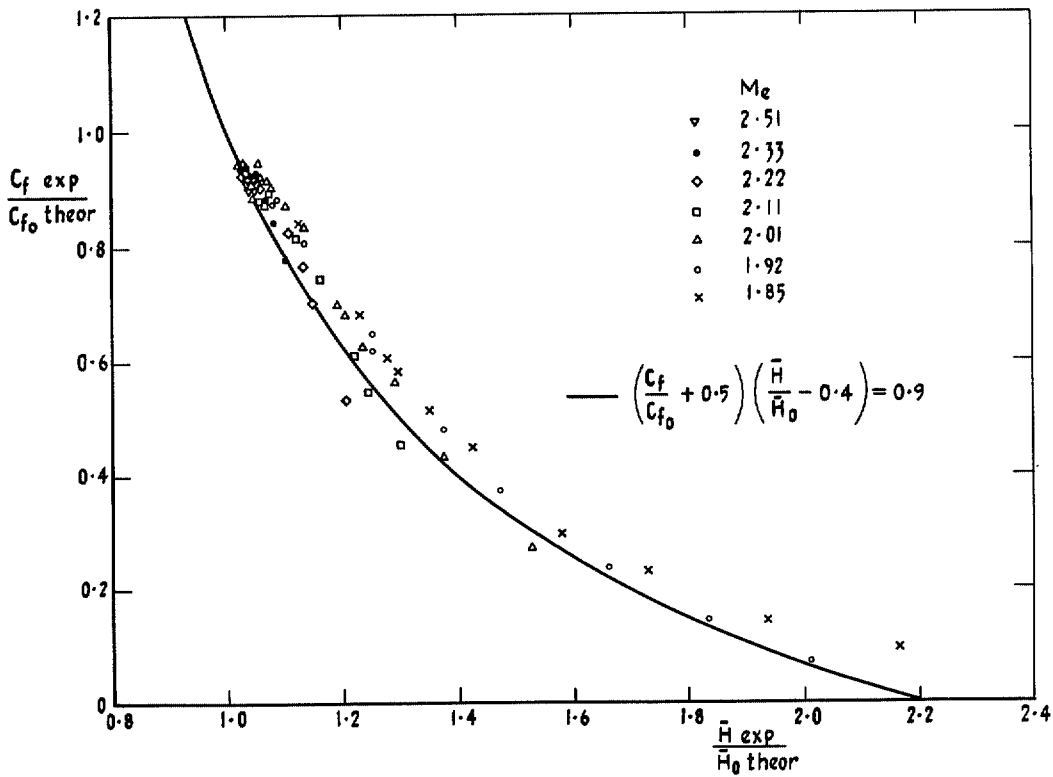


FIG. 4. Test of skin-friction relation in supersonic flow.

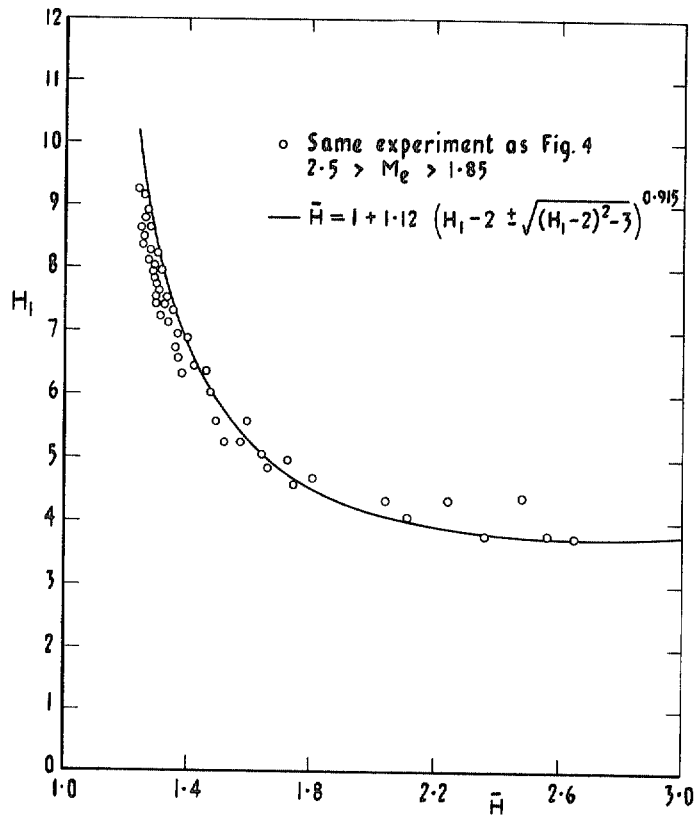


FIG. 5. Test of empirical $H_1(\bar{H})$ relation at supersonic speeds.

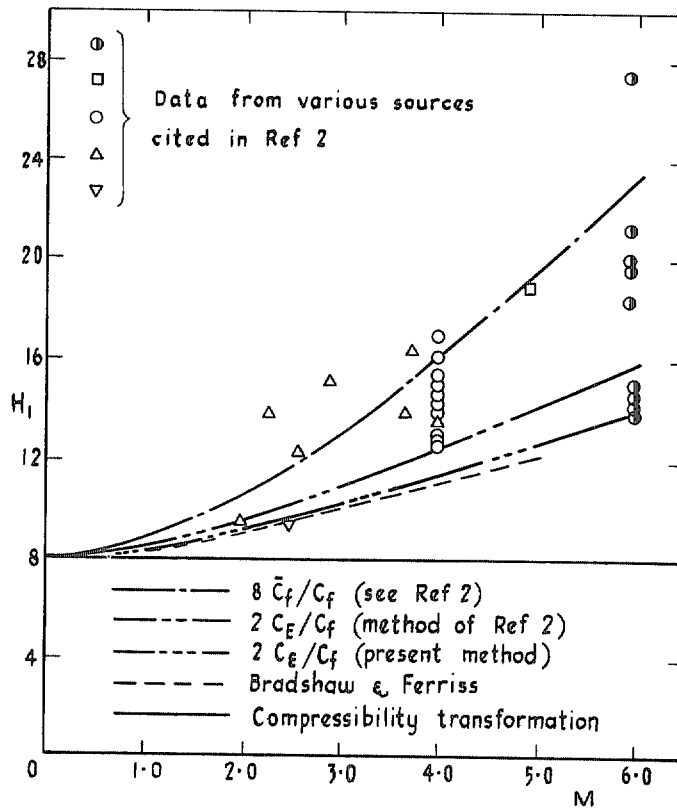


FIG. 6. Variation of H_1 with Mach number in adiabatic flows at constant pressure.

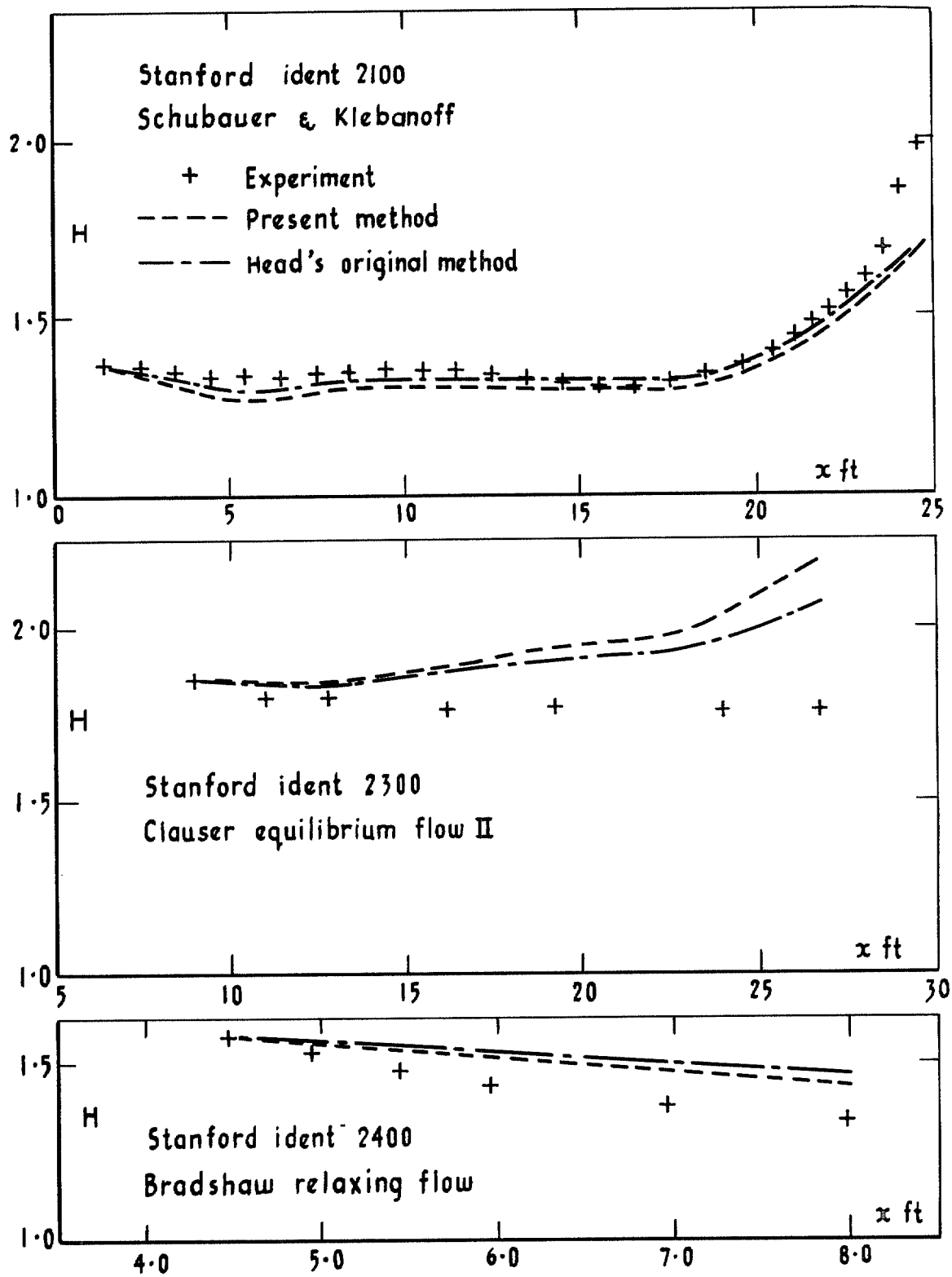


FIG. 7. Comparison between the present method, Head's original method and three Stanford test cases.

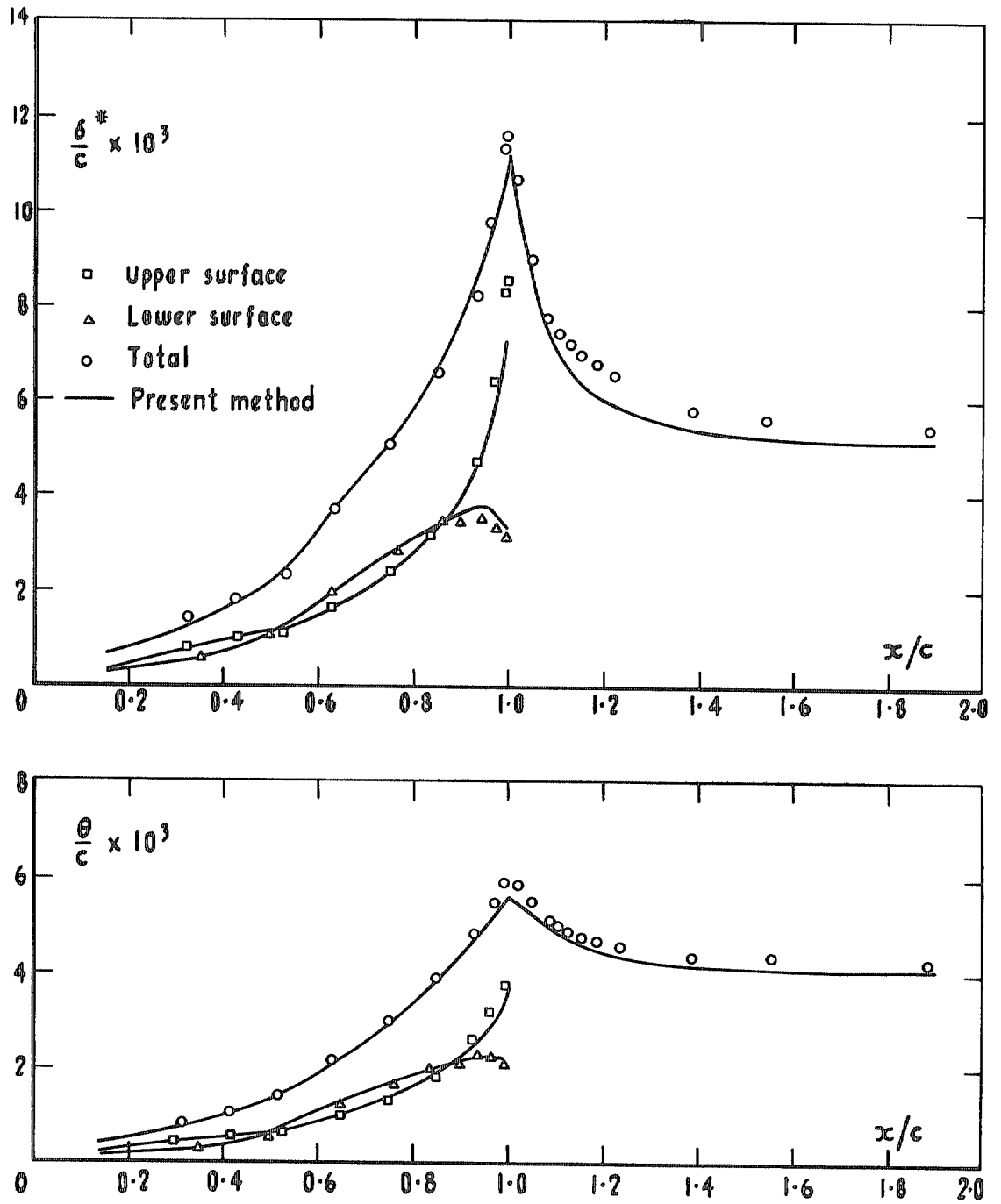


FIG. 8. Prediction of boundary layer and wake development on a lifting aerofoil at $M = 0.73$.

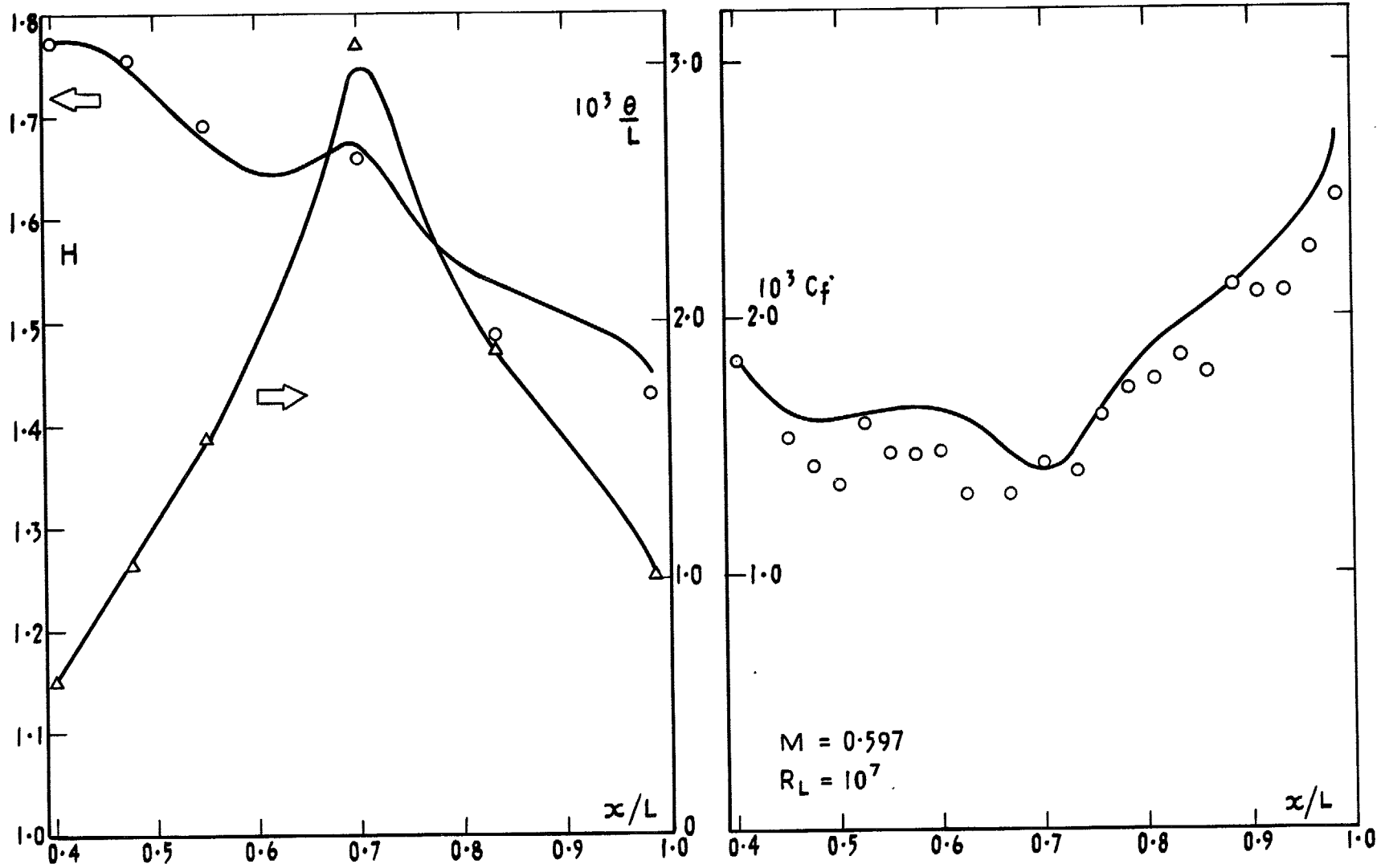


FIG. 9a. Prediction of boundary layer development on a waisted body of revolution at subsonic speed.

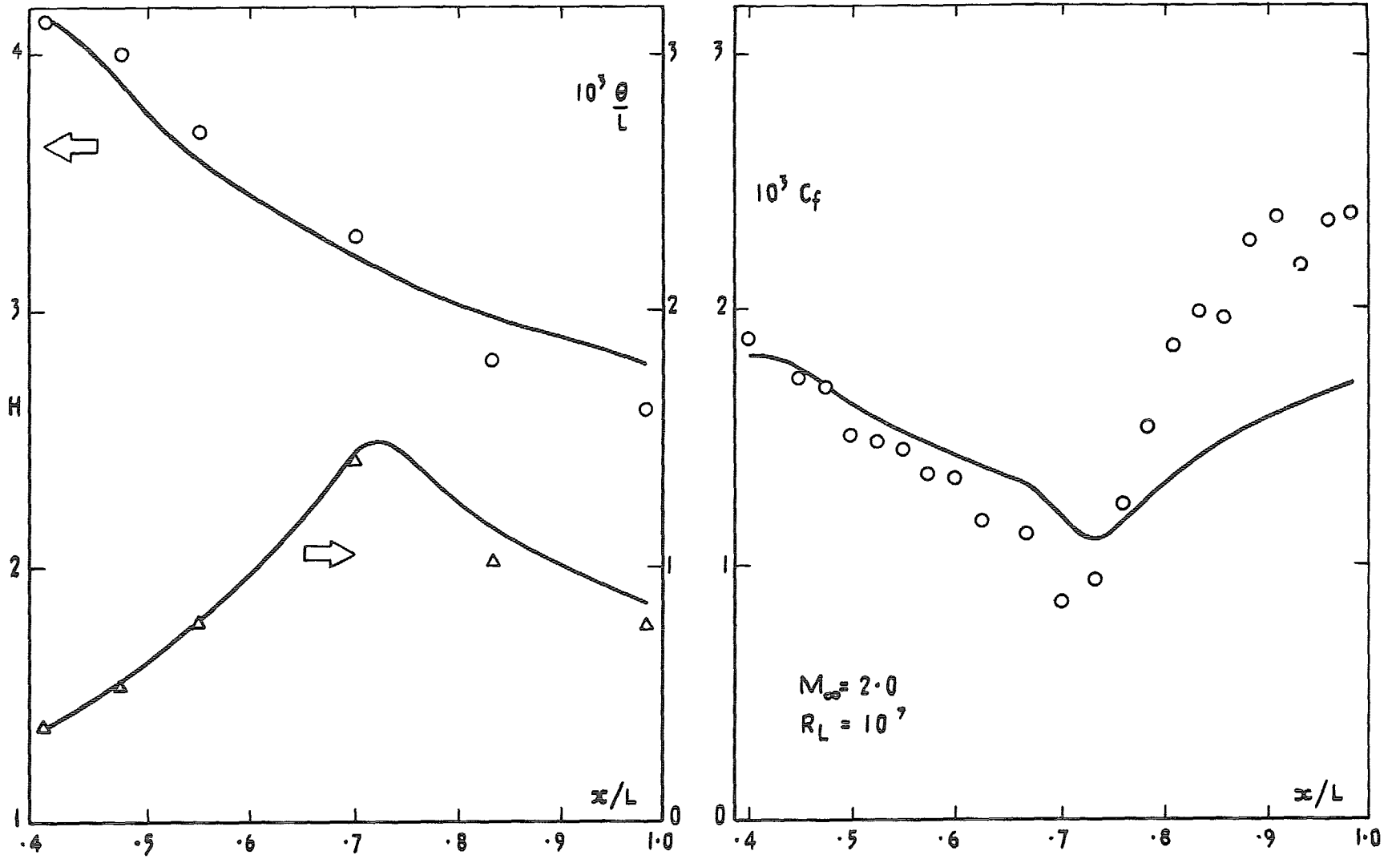


FIG. 9b. Prediction of boundary layer development on a waisted body of revolution at supersonic speed.

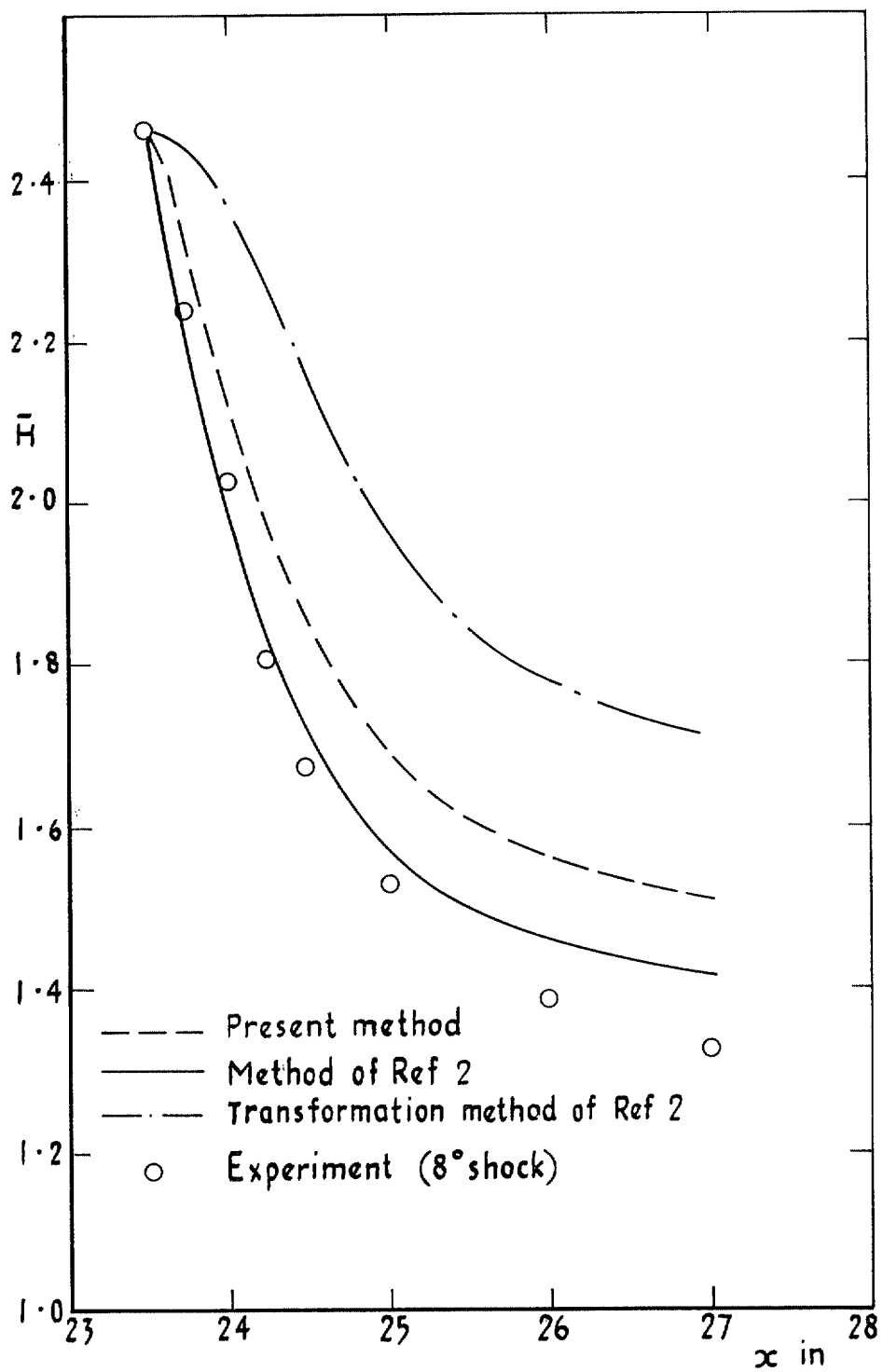


FIG. 10. Prediction of boundary layer recovery after interaction with an incident shock wave ($M \approx 2.0$).

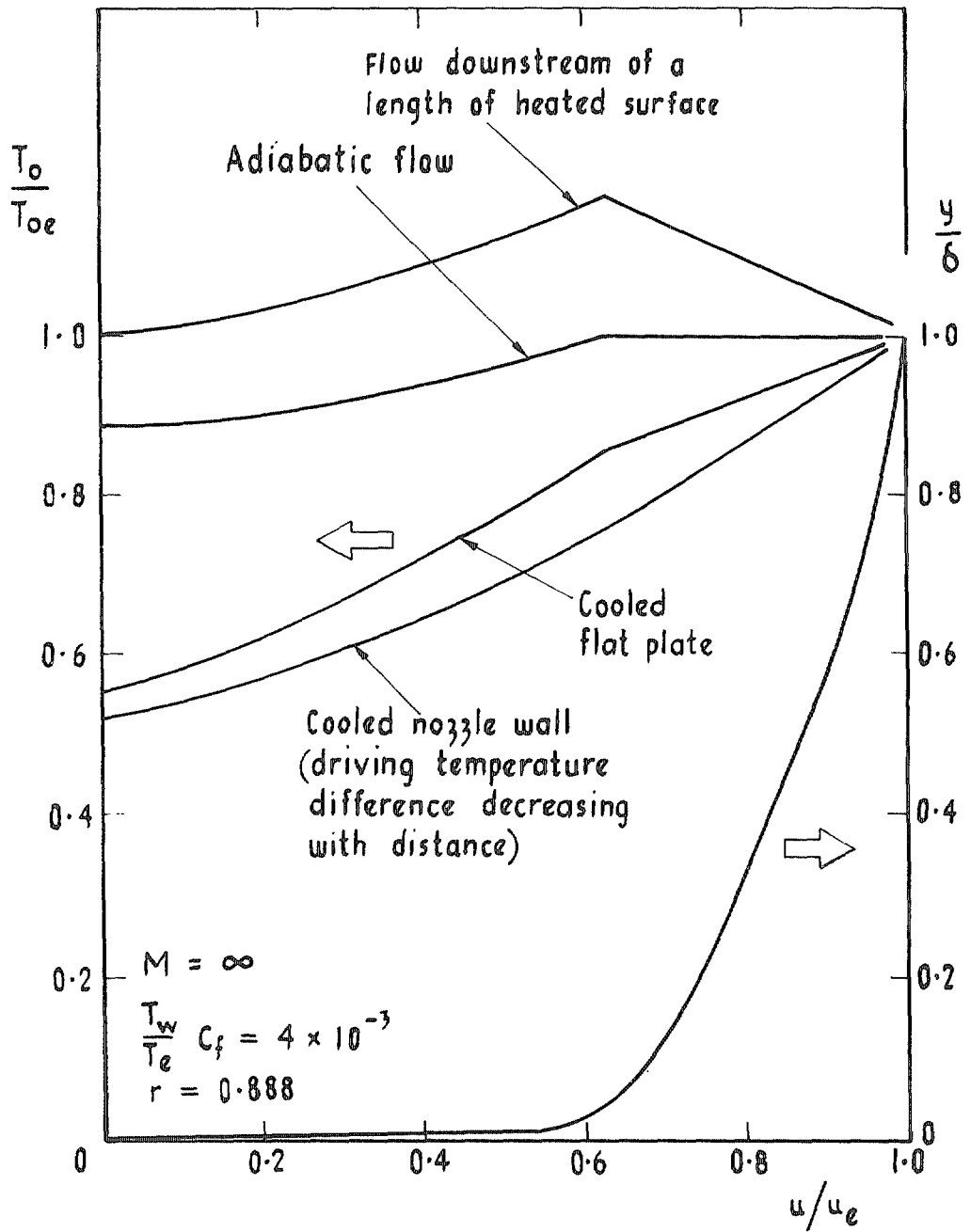


FIG. 11. Some hypothetical temperature/velocity polars.

R. & M. No. 3788

© Crown copyright 1976

HER MAJESTY'S STATIONERY OFFICE

Government Bookshops

49 High Holborn, London WC1V 6HB
13a Castle Street, Edinburgh EH2 3AR
41 The Hayes, Cardiff CF1 1JW
Brazennose Street, Manchester M60 8AS
Southey House, Wine Street, Bristol BS1 2BQ
258 Broad Street, Birmingham B1 2HE
80 Chichester Street, Belfast BT1 4JY

*Government publications are also available
through booksellers*

R. & M. No. 3788

ISBN 0 11 470959 9